Applied Physics B (2022) 128:212
https://doi.org/10.1007/s00340-022-07930-8

Applied Physics B
Lasers and Optics

RESEARCH

Doppler-free dual-excited state spectroscopy and its application for measurement of hyperfine structure of $6D_{5/2}$ level of ^{133}Cs

Baodong Yang[1,2,3] · Zhiyu Gou[1] · Junmin Wang[1,2,3] · Haitao Zhou[1]

Received: 16 August 2022 / Accepted: 18 October 2022

Abstract
Based on cesium $6S_{1/2}$—$6P_{3/2}$—$6D_{5/2}$ (852 nm + 917 nm) ladder-type system, we simultaneously obtain the Doppler-free saturated absorption spectroscopy (SAS) between the $6S_{1/2} \rightarrow 6P_{3/2}$ transition and optical–optical double resonance (OODR) spectroscopy between the $6P_{3/2} \rightarrow 6D_{5/2}$ transition, when the frequency of 852 nm laser is scanned over the lower transition while keeping the 917 nm laser resonant on the upper transition. The SAS as a frequency scale is used to measure the frequency intervals of hyperfine splitting of the $6D_{5/2}$ excited state via the OODR spectra. With the measured values of hyperfine splitting, the hyperfine coupling constants of the $6D_{5/2}$ state are determined as magnetic dipole $A_{hfs} = -4.60\ (5)$ MHz and electric quadrupole $B_{hfs} = 0.23\ (47)$ MHz, which are consistent with previous results. A simple and self-calibration method of measuring the unknown hyperfine structure of an excited state using its own known hyperfine splitting of another state is demonstrated without the aid of any extra frequency calibration tools.

1 Introduction

The research on high-precision spectroscopy of atomic hyperfine splitting is very important for understanding the atomic structure, and testing the fundamental physical constants and parity non-conservation [1–4]. In particular, hyperfine structures of alkali-metal atoms have been a subject of much theoretical and experimental attention for their simple energy level structure, as they are some hydrogen-like atoms with only one valence electron in their outermost shells. Hyperfine structure of atoms resulting from electron-nucleus interactions is sensitive to electron correlation effects, relativistic effects, and nuclear structure and so on [5, 6]. For the hyperfine structures of S and P states, the theoretical results are in good agreement with the experimental results [7, 8]. However, the theoretical predictions of hyperfine structures of the D state remain a challenge because of complex electron cloud distribution and strong correlation effects. Therefore, accurate measurement of the D state is particularly important for testing the computational treatment of correlation and clarifying the inconsistency between theoretical and experimental results [9, 10]. The hyperfine splitting frequency intervals of the D state are often anomalously small and even inverted, so it is critical to obtain the spectra between excited states with narrow linewidth and high signal-to-noise ratio for precise measurement [1]. With a room-temperature atomic vapor cell, Doppler-free two-photon spectroscopy [11–13], optical–optical double-resonance (OODR) absorption spectroscopy by the stepwise excitation process [14–16], double-resonance optical pumping (DROP) spectroscopy [17–22], and electromagnetically induced transparency (EIT) spectroscopy [23, 24], and two-color polarization spectroscopy [25–28] in a ladder-type atomic system are popularly adopted to obtain the information about the hyperfine splitting structure of D state, which are then measured using some extra frequency calibration tools such as an electro-optic phase modulator (EOM) [11, 14, 22], an acousto-optic modulator (AOM) [12, 21], frequency comb [13, 15, 16, 18], Fabry–Perot cavity [19, 20] and so on, and further people use these measured values to determine the magnetic dipole coupling constant (A_{hfs}) and electric quadrupole coupling constant (B_{hfs}). To obtain high-resolution excited state spectra, Georgiades et al. measured the hyperfine coupling constants A_{hfs} and B_{hfs} of

✉ Baodong Yang
ybd@sxu.edu.cn

[1] College of Physics and Electronic Engineering, Shanxi University, Taiyuan 030006, China

[2] State Key Laboratory of Quantum Optics and Quantum Optics Devices and Institute of Opto-Electronics, Shanxi University, Taiyuan 030006, China

[3] Collaborative Innovation Center of Extreme Optics, Shanxi University, Taiyuan 030006, China

Published online: 31 October 2022

^{133}Cs $6D_{5/2}$ excited state using the two-photon spectroscopy in a magneto-optical trap for the almost-Doppler-free environment [29]. Fort et al. also measured the hyperfine splitting of excited states $8S_{1/2}$, $6D_{3/2}$, and $6D_{5/2}$ of ^{133}Cs with OODR spectroscopy in trapped cesium atoms [30].

In this work, based on a ladder-type atomic system, we develop an experimental technique of dual-excited state spectroscopy, and demonstrate a simple and robust method for measuring the hyperfine structure of higher excited state using the known hyperfine frequency intervals of intermediate excited state instead of some extra frequency calibration devices, and giving the hyperfine coupling constants A_{hfs} and B_{hfs} of the higher excited state.

2 Theory and experimental setup

The hyperfine splitting structure is generally derived from the interaction of the nuclear magnetic dipole moment with the magnetic flux density created by electrons, and the interaction of the electric quadrupole moment with the gradient of the electric field at the nucleus. The frequency interval of adjacent hyperfine levels due to the nuclear spin is given by [14, 22]:

$$\Delta E_{hfs}(F \to F-1) = A_{hfs}F + B_{hfs}\frac{\frac{3}{2}F\left[F^2 - I(I+1) - J(J+1) + \frac{1}{2}\right]}{I(2I-1)J(2J-1)} \quad (1)$$

where I and J are the quantum numbers for the nuclear spin angular momentum and the total electronic angular momentum, and $F = I + J$ is the total angular momentum quantum number of atoms. A_{hfs} and B_{hfs} are the magnetic dipole and electric quadrupole coupling constants, respectively. Thus Eq. (1) can be used to determine A_{hfs} and B_{hfs} through the measured hyperfine intervals.

Figure 1 shows the relevant hyperfine energy levels of the ^{133}Cs $6S_{1/2}$—$6P_{3/2}$—$6D_{5/2}$ transitions. For the ^{133}Cs, $I = 7/2$. The hyperfine splitting of the ground state $6S_{1/2}$ is 9192.631770 MHz, and has been used as the definition of a second. The splitting intervals between the hyperfine levels $F' = 2, 3, 4, 5$ of the intermediate state $6P_{3/2}$ with natural linewidth $\Gamma_1 = 5.2$ MHz are 151.225, 201.287, 251.092 MHz, respectively [31, 32]. The higher excited state $6D_{5/2}$ with natural linewidth $\Gamma_2 = 3.1$ MHz is splitted into six hyperfine levels F" = 1–6 [14, 29].

The schematic of experimental setup is depicted in Fig. 2. A homemade 852 nm external cavity diode laser (ECDL) with a typical linewidth ~ 800 kHz can be tuned to either 852.335 nm for the $6S_{1/2}$ (F = 3) → $6P_{3/2}$ (F' = 2, 3, 4) transitions, or 852.356 nm for the $6S_{1/2}$ (F = 4) → $6P_{3/2}$ (F' = 3, 4, 5) transitions. When the 852 nm laser frequency is scanned, Doppler-free saturated absorption spectroscopy (SAS) with

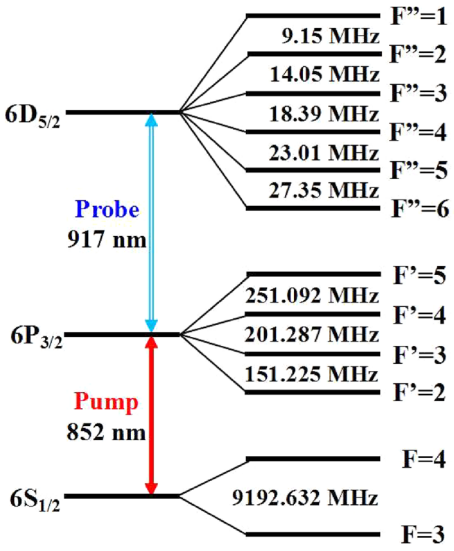

Fig. 1 The hyperfine energy levels of ^{133}Cs for the $6S_{1/2}$—$6P_{3/2}$—$6D_{5/2}$ transitions

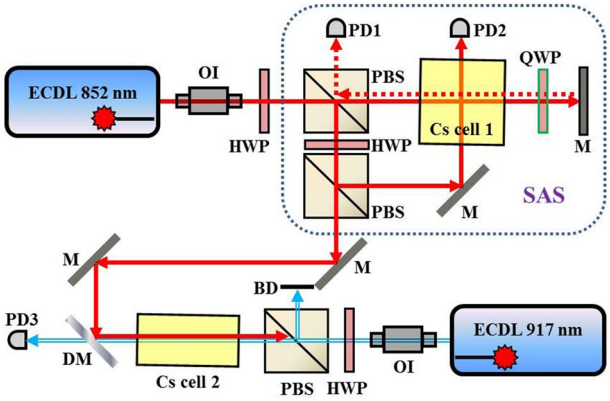

Fig. 2 Experimental setup for the measurement of the hyperfine splitting structure of the $6D_{5/2}$ state of ^{133}Cs, and the saturated absorption spectroscopy device is highlighted by a dotted box. (*ECDL* external cavity diode laser, *OI* optical isolator, *HWP* half-wave plate, *QWP* quarter-wave plate, *PBS* polarizing beam splitter, *M* mirror, *PD* photodiode, *Cs cell* cesium vapor cell, *SAS* saturated absorption spectroscopy, *DM* dichroic mirror, *BD* beam dump.)

a flat background is obtained as the difference between the PD1 and PD2 voltages in the Cs cell 1 (a cube with 25 mm edges), just for the convenience of building a precision frequency scale by determining the exact position of SAS signals using multi-peak Lorentz fitting in our measurement of the ^{133}Cs $6D_{5/2}$ hyperfine structure. The frequency scanning 852 nm laser simultaneously acts as a pump laser, and populates atoms into the intermediate state $6P_{3/2}$ from the ground state $6S_{1/2}$, while the 917 nm laser as probe laser operated between the excited states $6P_{3/2}$ and $6D_{5/2}$ transition line (no scanning), and an OODR spectrum in PD3 detector

is obtained under the two-photon resonance condition. To get a narrow linewidth and high-resolution OODR spectrum taking advantage of the atomic coherence effect in a ladder-type system [23, 24], the pump and probe laser beams are counter-propagating in the Cs cell 2 at room temperature via a dichroic mirror (DM). The Cs cell 2 with 10 cm long has been wrapped with three layers of μ-metal sheets to reduce the influence of stray Earth's magnetic field, and a residual magnetic field is less than ~ 20 mG. The pump and probe beams are about ~ 1.6 mm in diameter, and their power are ~ 24 μW and ~ 16 μW, corresponding to Rabi frequencies of ~ 3.1 MHz and ~ 2.2 MHz, respectively. The polarizations of both beams in the Cell 2 are linear and parallel to each other. Finally, the SAS between the $6S_{1/2}$—$6P_{3/2}$ transition and OODR spectrum between the $6P_{3/2}$—$6D_{5/2}$ transition are simultaneously obtained. With the known hyperfine frequency intervals of the $6P_{3/2}$ state in SAS as a frequency reference, the time axis of OODR spectrum recorded by a digital oscilloscope is linearly translated into the frequency axis for the measurement of the hyperfine structure of the $6D_{5/2}$ excited state.

3 Results and discussion

3.1 Characteristic of traditional OODR spectroscopy

Figure 3 shows traditional OODR spectra when the frequency of the 852 nm pump laser is locked one by one to the three resonance peaks and two crossover (CO) peaks of the SAS between $6S_{1/2}$ (F = 4) → $6P_{3/2}$ transition, and the 917 nm probe laser is scanned over the whole $6P_{3/2} \rightarrow 6D_{5/2}$ transition. Horizontal x axis is calibrated by the known frequency interval values of $6D_{5/2}$ state provided by Ref [11], and its frequency detuning is relative to the $6P_{3/2}$ (F' = 5) → $6D_{5/2}$ (F" = 6) resonance in Fig. 3. Under the condition of two-photon resonance considering the Doppler effect ($\Delta_{pump} + \nu/c*\upsilon_{pump} + \Delta_{probe} - \nu/c*\upsilon_{probe} = 0$, Δ_{pump} and Δ_{probe} are frequency detuning of pump laser and probe laser, υ_{pump} and υ_{probe} are frequency of pump laser and probe laser, ν is the speed of atoms in the direction of the laser beams, c is speed of light), these spectral signals from left to right correspond in turn to the hyperfine transitions between the energy levels F'–F" = 5–6, 5–5, 4–5, 5–4, 4–4, 3–4, 4–3, 3–3, 3–2 as shown in Fig. 3. It is clear that the frequency intervals of OODR spectra are insensitive to frequency changes of the 852 nm pump laser: when pump laser resonates at different frequency positions between the $6S_{1/2}$(F = 4)-$6P_{3/2}$ transition, it only results in a shift of the OODR spectrum as a whole and a change in the relative amplitude of these signals, while maintaining the same frequency intervals. For example, when the pump laser is resonant on the F-F' = 4–5 transition, more atoms with zero velocity in the direction of pump laser beam are populated in the F' = 5 hyperfine state, so the signals for the F'–F" = 5–6, 5–5, 5–4 transitions are relatively bigger. Similarly, while the pump laser is tuned to the side of the F-F' = 4–3 transition, the signals for the F'–F" = 3–4, 3–3, 3–2 will gradually grow big. The above experimental results corroborate that the frequency intervals in the OODR spectrum are immune to frequency drift of the 852 nm pump laser, it is advantageous for precise measurement of the hyperfine structure of higher excited states $6D_{5/2}$. However, using the traditional OODR spectrum to measure the hyperfine structure of the excited state, some extra frequency calibration tools are required, such as EOM, AOM, frequency comb, etc. [11–22].

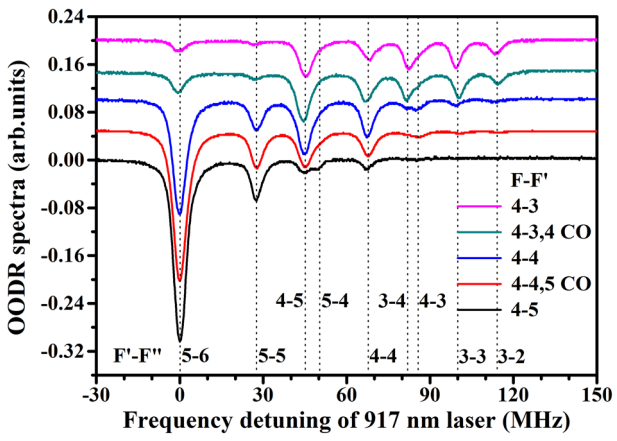

Fig. 3 Traditional optical–optical double resonance (OODR) spectra when the frequency of 852.3 nm pump laser is resonance on one of the $6S_{1/2}$ (F = 4) → $6P_{3/2}$ (F' = 3–5) hyperfine transitions, respectively

3.2 Dual-excited state spectroscopy and measurement of the hyperfine structure of the higher excited state

The method for obtaining dual-excited state spectroscopy in a ladder-type atomic system is as follows: First, we obtain traditional OODR spectra (Fig. 3) by locking the 852 nm pump laser to the one of hyperfine transitions between the $6S_{1/2}$ and $6P_{3/2}$ states, while keeping 917 nm probe laser scanning over the whole $6P_{3/2} \rightarrow 6D_{5/2}$ transition; and then decrease the scanning range of 917 nm laser to zero, and keep the 917 nm laser resonant with one position between the $6P_{3/2} \rightarrow 6D_{5/2}$ transition with the help of traditional OODR spectra; finally, the 852 nm pump laser is scanned over the $6S_{1/2} \rightarrow 6P_{3/2}$ transition.

Obviously, the above approach is different from the traditional OODR technique [14, 16]: for the first time, we adopt the completely inverse working mode of two lasers: the 852 nm pump laser is scanned over the lower transition by a piezoelectric ceramic transducer (PZT) driving the grating of ECDL with the ~ 20 Hz scanning frequency,

while the 917 nm probe laser is resonant on the different frequency position in the upper transition, the OODR spectra with a completely flat background for characterizing hyperfine structure of the $6D_{5/2}$ excited state are also obtained in detector PD3 under the condition of two-photon resonance as shown in Fig. 4. Moreover, due to the frequency scanning of the 852 nm pump laser, the SAS with linewidth of about ten or twenty MHz for the $6S_{1/2}$ (F = 4) → $6P_{3/2}$ transition is obtained as the differential signal between PD1 and PD2 detectors simultaneously, which can be as a frequency calibration tool with the known hyperfine splitting frequency intervals of the $6P_{3/2}$ excited state as shown in Fig. 1 [31, 32], and its detuning is set to the $6S_{1/2}$(F = 4) → $6P_{3/2}$(F' = 5) resonance transition in Fig. 4. When the frequency of 917 nm probe laser is tuned between the $6P_{3/2}$—$6D_{5/2}$ transition, it only causes an overall shift of the OODR spectrum indicated by lines 1–4 from top to bottom, which is similar to the Fig. 3, and also shows that the frequency intervals of OODR spectra are insensitive to frequency drift of the 917 nm probe laser.

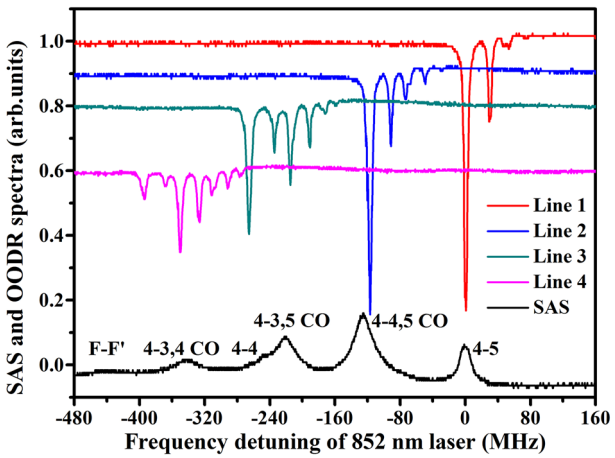

Fig. 4 Dual-excited state spectroscopy of the $6D_{5/2}$ and $6P_{3/2}$ states. The color lines 1–4 from top to bottom represent OODR spectra when the frequency of 917 nm probe laser is resonant on the different frequency position between the $6P_{3/2}$ → $6P_{5/2}$ transition, while the frequency of 852 nm pump laser is scanned over the $6S_{1/2}$ (F = 4) → $6P_{3/2}$ transition. The SAS curve as a frequency reference

The higher excited state energy levels of an atom are, the smaller their hyperfine splittings are, and so it is key to fully distinguish hyperfine energy levels experimentally. In a ladder-type atomic system, the linewidth of excited state spectroscopy is usually more narrow when the pump and probe laser beams are counter-propagating through the atomic medium in a room-temperature vapor cell due to the atomic coherence effect [23, 24]. Theoretically, the natural linewidth for two-color excited state spectrum under the condition of weak laser fields is given by [33]:

$$\Gamma = \Gamma_2 + \left|\frac{K_1 - K_2}{K_1}\right|\Gamma_1 \tag{2}$$

where k_1 and k_2 are the wave vectors of the pump laser and probe laser, respectively. Using the $\Gamma_1 = 5.2$ MHz natural linewidth of the $6P_{3/2}$ state and the $\Gamma_2 = 3.1$ MHz of the $6D_{5/2}$ state, Eq. (2) predicts the natural linewidth of the excited state spectrum of ~ 3.67 MHz. In our experiment, all spectral lines allowed by dipole selection rules between the excited states $6P_{3/2}$ and $6D_{5/2}$ in OODR spectrum are clearly distinguishable as shown in Fig. 5, and the narrowest spectral linewidth is about ~ 4.0 MHz, which is much smaller than that for co-propagating pump and probe laser beams in a ^{133}Cs vapor cell [14]. Thus, it is convenient that four frequency intervals of the hyperfine splitting for the $6D_{5/2}$ state can be simultaneously determined in a single measurement.

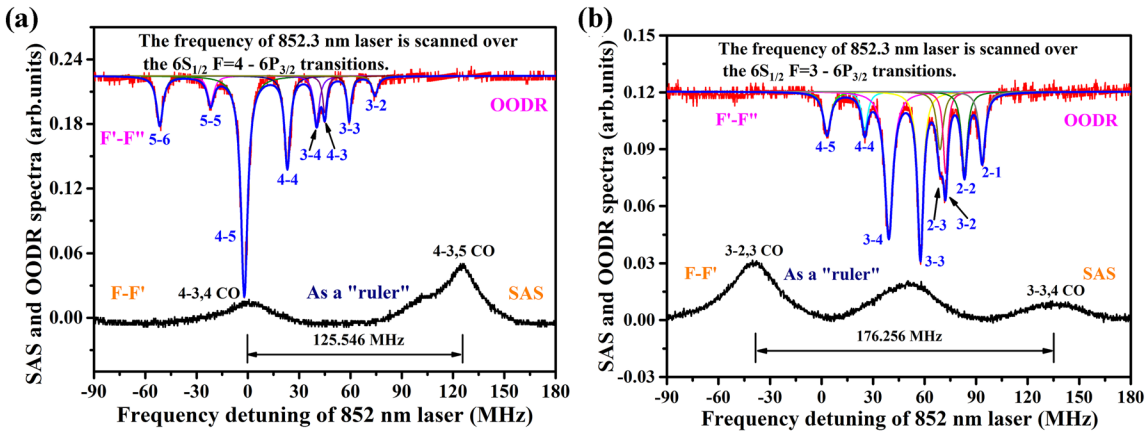

Fig. 5 Measurement of the hyperfine splitting structure for the excited state $6D_{5/2}$ of ^{133}Cs when the frequency of 852.3 nm laser is scanned over the $6S_{1/2}$F = 4 → $6P_{3/2}$ (**a**) and $6S_{1/2}$F = 3 → $6P_{3/2}$ (**b**) transitions, respectively. The colored solid lines display multi-peak Lorentz fitting while the red curve with noise displays the OODR spectrum, and the black line at the bottom represents the SAS as a frequency ruler

To minimize the influence of nonlinear frequency scanning of a grating external cavity on measurement accuracy, the frequency scanning range of the 852.3 nm pump laser is reduced as much as possible, and only a complete set of OODR spectra between the excited states $6P_{3/2} \rightarrow 6D_{5/2}$ transition can be obtained as shown in Fig. 5. When the frequency of 852.3 nm pump laser is scanned over the $6S_{1/2}F = 4 \rightarrow 6P_{3/2}$ transition, the known 125.546 MHz frequency interval between the $F = 4 \rightarrow F' = 3,4$ and $F = 4 \rightarrow F' = 3,5$ crossover resonance peaks of the SAS is used to calibrate the horizontal axis of OODR spectrum by the multi-peak Lorentz function fitting to determine the exact position of SAS signals. Then we again use multi-peak Lorentz curves to fit the OODR spectra to locate the central position of each signal as shown in Fig. 5(a), and calculate the frequency intervals between them. Finally, considering the influence of wavelength mismatch between the pump and probe laser in a ladder-type atomic system, these values of frequency intervals are multiplied by a k_2/k_1 factor to get the hyperfine intervals between the $F'' = 6–2$ of the $6D_{5/2}$ state. Due to the limitation of the transition selection rule $\Delta M_F = \pm 1$, to get the frequency interval between the $F'' = 2$ and $F'' = 1$ of the $6D_{5/2}$ state, the 852.3 nm laser is again scanned over the $6S_{1/2}F = 3 \rightarrow 6P_{3/2}$ transition, we use the known 176.256 MHz frequency interval between the $F = 3 \rightarrow F' = 2,3$ and $F = 3 \rightarrow F' = 3,4$ crossover resonance peaks of the SAS to calibrate the horizontal axis of OODR spectrum in Fig. 5(b). Each hyperfine splitting interval of the $6D_{5/2}$ state is averaged over 30—40 individual spectra, and their histograms at bin size 0.3—0.4 MHz of the hyperfine splitting values with corresponding normal distribution curves are shown in Fig. 6. Table 1 shows good agreement between our measured hyperfine splitting intervals of the $6D_{5/2}$ state and that of previous literatures [11, 13, 14, 30].

For any one measurement, measuring accuracy mainly depends on two factors: one is the clearness of the measured object, and another is the precision of measurement tools. In our experiment, the OODR spectra as the measured object should be enough in narrow linewidth、high resolution and high signal-to-noise ratio; although the linewidth of SAS as a frequency calibration is somewhat broad, by the processing of the same experimental data repeatedly, the statistical error in determining the exact position of SAS and OODR spectral lines by multi-peak Lorentz fitting is < ~0.10 MHz.

Another possible error comes from the light shift, which is proportional to the laser intensity. In our experiment, Autler-Townes splitting of hyperfine components is easily observed in the OODR spectrum when the intensity of 852.3 nm pump laser increases. But in measurement, the power of the 852.3 nm pump laser is low enough based on the fact that the linewidth of obtained OODR spectrum is very narrow and close to the theoretical prediction value [14, 33]. Furthermore, the polarizations of the pump and probe

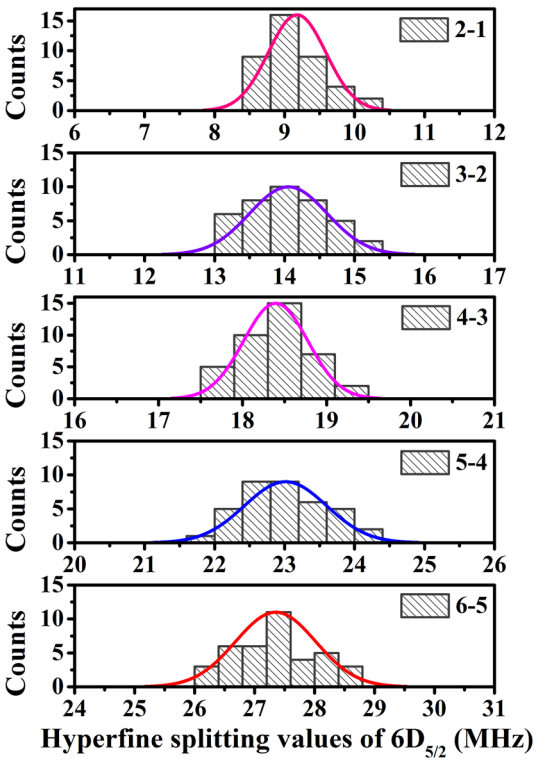

Fig. 6 Histograms of hyperfine splitting values with corresponding normal distribution curves for the excited state $6D_{5/2}$ of ^{133}Cs

beams are linear utilizing PBS cubes with an extinction ratio of > 1000:1, which has little effect on the center of OODR spectral signals [12]. So the influence of the light shift as a systematic error is negligible. In addition, the Zeeman shift due to the residual magnetic field is estimated to be less than ~ 0.04 MHz, which is also negligible. The other source of systematic error, such as pressure (collisional) shift for a room-temperature vapor cell, and pulling effect due to spectral overlap from the neighboring transitions for our narrow-linewidth OODR spectra, will be smaller [12].

At present, the experimental error in the measurement of frequency intervals mainly results from the nonlinear frequency scanning of our homemade 852.3 nm pump laser, a high-quality PZT driving the grating of ECDL will further improve the measuring accuracy of the hyperfine structure.

3.3 Determination of magnetic dipole and electric quadrupole coupling constants

Using Eq. (1) and the above measured hyperfine splitting values of the $6D_{5/2}$ state ($I = 7/2$ and $J = 5/2$) as shown in Table 1, a set of coupled linear equations are obtained:

$6A_{hfs} + 18/35B_{hfs} = -27.35\ (67)$ MHz.

$5A_{hfs} + 1/28B_{hfs} = -23.01\ (59)$ MHz.

$4A_{hfs} - 8/35B_{hfs} = -18.39\ (38)$ MHz.

Table 1 Measured values of hyperfine splitting of the excited state $6D_{5/2}$ for the ^{133}Cs

Hyperfine intervals of the $6D_{5/2}$ state	Measured (this work) (MHz)	Ref. [11] (MHz)	Ref.[13][a] (MHz)	Ref [14] (MHz)	Ref. [30] (MHz)
F" = 1 → F" = 2	9.15 (37)	8.97 (39)	9.23	9.4 (2)	-
F" = 2 → F" = 3	14.05 (56)	14.07 (36)	13.85	14.8 (2)	-
F" = 3 → F" = 4	18.39 (38)	18.57 (21)	18.49	18.5 (2)	-
F" = 4 → F" = 5	23.01 (59)	22.40 (8)	23.15	23.1 (2)	22.1 (7)
F" = 5 → F" = 6	27.35 (67)	27.93 (35)	27.82	27.5 (1)	29.1 (5)

[a]Values of hyperfine splitting have been calculated from the reported A_{hfs} and B_{hfs} values

Table 2 The magnetic dipole (A_{hfs}) and electric quadrupole (B_{hfs}) hyperfine coupling constants of the $6D_{5/2}$ state for the ^{133}Cs

State	Reference	Method	A_{hfs} (MHz)	B_{hfs} (MHz)
^{133}Cs $6D_{5/2}$	2022, This work	Dual-excited state spectroscopy (self-calibration)	− 4.60 (5)	0.23 (47)
	2021, Herd et al.[13]	Two-photon spectroscopy + frequency comb	− 4.629 (14)	− 0.10 (15)
	2006, Kortyna et al.[14]	OODR + EOM	− 4.66 (4)	0.9 (8)
	2005, Ohtsuka et al.[11]	Two-photon spectroscopy + EOM	− 4.56 (9)	− 0.35 (18)
	1994, Georgiades et al.[29]	Two-photon spectroscopy in cold atoms + AOM	− 4.69 (4)	0.18 (73)
	1975, Tai et al.[1]	Cascade fluorescence spectroscopy + decoupling	− 3.6 (10)	–

$$\begin{aligned} 3A_{hfs} - 9/28B_{hfs} &= -14.05\ (56)\ \text{MHz} \\ 2A_{hfs} - 2/7B_{hfs} &= -9.15(37)\ \text{MHz} \end{aligned} \tag{3}$$

Applying the method of least squares, we determine the magnetic dipole coupling constant A_{hfs} and electric quadrupole coupling constant B_{hfs}, and propagate the uncertainties through these formulas. The A_{hfs} agrees well with previous reports, as shown in Table 2. However, the consistency of B_{hfs} is poor in different literature due to its small influence on the hyperfine splitting of $6D_{5/2}$ state by indicated Eqs. (3), which can be seen as the ratio of coefficients of B_{hfs} and A_{hfs} ranges from 1/28: 5 = 0.7% to 2/7: 2 = 14%.

4 Conclusions

We have demonstrated a robust and self-calibration method of measuring the unknown hyperfine structure of one excited state using the known hyperfine splitting interval of another excited state in a ladder-type atomic system. Based on the ^{133}Cs $6S_{1/2}$—$6P_{3/2}$—$6D_{5/2}$ (852 nm + 917 nm) system, we have confirmed that the relative positions of these two-color absorption signals in OODR spectra between the $6P_{3/2} \rightarrow 6D_{5/2}$ transition are immune to the frequency drift of the 852 nm or 917 nm lasers in two different laser scanning modes, which is beneficial for precise determination of the hyperfine splitting intervals of excited states. The OODR spectrum with narrow linewidth using the atomic coherence effect is obtained when adopting the counter-propagting pump and probe laser beams in a room-temperature ^{133}Cs vapor cell [27], this is helpful to fully distinguish the hyperfine splitting structure of higher excited states. Without any extra frequency calibration tools, all five hyperfine splitting intervals of the $6D_{5/2}$ excited state are measured using the Doppler-free SAS spectrum with the known hyperfine splitting intervals of excited state $6P_{3/2}$ as a frequency scale. Hyperfine coupling constants of the $6D_{5/2}$ excited state are theoretically calculated with our measured frequency intervals: A_{hfs} = -4.60 (5) MHz, B_{hfs} = 0.23 (47) MHz, agreeing with the reported measurements [11, 13, 14, 29], and confirming the feasibility of our measuring approach, which can also be used to explore the hyperfine structure of some other higher excited states.

Author contributions Baodong Yang designed and performed the experiment, and wrote the paper. Zhiyu Gou dealt with the experimental data. Junmin Wang and Haitao Zhou gave useful discussion, and corrected the paper.

Funding Funding for this research was supported by the National Natural Science Foundation of China, Grant Nos. 61975102, and 11974226; the Natural Science Foundation of Shanxi Province, Grant No. 20210302123437; the National Key Research and Development Program of China, Grant No. 2017YFA0304502; and the Scientific and

Technological Innovation Programs of Higher Education Institutions in Shanxi Province, Grant No. 2019L0101.

Declarations

Conflict of interest The authors declare no competing interests.

References

1. C. Tai, W. Happer, R. Gupta, Hyperfine structure and lifetime measurements of the second-excited D states of rubidium and cesium by cascade fluorescence spectroscopy. Phys. Rev. A **12**(3), 736–747 (1975)
2. N. Leefer, A. Cingöz, D. Budker, Measurement of hyperfine structure and isotope shifts in the Dy 421 nm transition. Opt. Lett. **34**(17), 2548–2550 (2009)
3. P.V. Kiran Kumar, B. Nisheeth, M. Sankari, M.V. Suryanarayana, Precision measurement of the hyperfine structure of $8d^2D_{3/2}$ state of ^{133}Cs by the radio-frequency phase modulation technique, Opt. Commun. **320**, 77–83 (2014)
4. A. Chakrabarti, A. Ray, Exploring hyperfine levels of non-Rydberg excited states in a Ξ system using Autler-Townes splitting. Appl. Opt. **59**(3), 735–741 (2020)
5. O.N. Elijah, S. Dangka, N. Vasant, P. Kanhaiya, Hyperfine measurement of the $6P_{1/2}$ state in ^{87}Rb using double resonance on blue and IR Transition. J. Phys. B **53**(9), 095001 (2020)
6. S. Pucher, P. Schneeweiss, A. Rauschenbeutel, A. Dareau, Lifetime measurement of the cesium $5^2D_{5/2}$ state. Phys. Rev. A **101**(4), 042510 (2020)
7. G.H. Jang, M. Na, B. Moon, T.H. Yoon, Absolute frequency measurement of the 6s6p $^1P_1$-6s7s $^1S_0$ transition of ^{174}Yb in a Yb hollow-cathode lamp. Phys. Rev. A **89**(6), 062510 (2014)
8. Y.N. Ren, B.D. Yang, J. Wang, G. Yang, J.M. Wang, Measurement of the magnetic dipole hyperfine constant A_{hfs} of cesium $7S_{1/2}$ state. Acta Phys. Sin. **65**(7), 073103 (2016)
9. Y.C. Lee, Y.H. Chang, Y.Y. Chang, Y.Y. Chen, C.C. Tsai, H.C. Chui, Hyperfine coupling constants of cesium 7D states using two-photon spectroscopy. Appl. Phys. B **105**, 391–397 (2011)
10. T.J. Chen, J.E. Chen, H.H. Yu, T.W. Liu, Y.F. Hsiao, Y.C. Chen, M.S. Chang, W.Y. Cheng, Absolute frequency of cesium $6S_{1/2}$-$6D_{3/2}$ hyperfine transition with a precision to nuclear magnetic octupole interaction. Opt. Lett. **43**(9), 1954–1957 (2018)
11. T. Ohtsuka, N. Nishimiya, T. Fukuda, M. Suzuki, Doppler-free two-photon spectroscopy of $6S_{1/2}$-$6D_{3/2,5/2}$ transition in cesium. J. Phys. Soc. Jpn. **74**(9), 2487–2491 (2005)
12. P. V. Kiran Kumar, M. Sankari, M. V. Suryanarayana, Hyperfine structure of the 7d $^2D_{3/2}$ level in cesium measured by Doppler-free two-photon spectroscopy, Phys. Rev. A **87**(1), 012503 (2013)
13. M.T. Herd, E.C. Cook, W.D. Williams, Absolute frequency measurement of the $6D_{5/2}$ level of neutral ^{133}Cs using two-photon spectroscopy. Phys. Rev. A **104**(4), 042812 (2021)
14. A. Kortyna, N.A. Masluk, T. Bragdon, Measurement of the $6d^2D_J$ hyperfine structure of cesium using resonant two-photon sub-Doppler spectroscopy. Phys. Rev. A **74**(2), 022503 (2006)
15. J.E. Stalnaker, V. Mbele, V. Gerginov, T.M. Fortier, S.A. Diddams, L. Hollberg, C.E. Tanner, Femtosecond frequency comb measurement of absolute frequencies and hyperfine coupling constants in cesium vapor. Phys. Rev. A **81**(4), 043840 (2010)
16. A. Nishiyama, S. Yoshida, Y. Nakajima, H. Sasada, K. Nakagawa, A. Onae, and K. Minoshima, Doppler-free dual-comb spectroscopy of Rb using optical-optical double resonance technique, Opt. Express **24**(22), 25894–25904 (2016)
17. H.S. Moon, W.K. Lee, L. Lee, J.B. Kim, Double resonance optical pumping spectrum and its application for frequency stabilization of a laser diode. Appl. Phys. Lett. **85**(18), 3965–3967 (2004)
18. H.S. Moon, W.K. Lee, H.S. Suh, Hyperfine-structure-constant determination and absolute-frequency measurement of the Rb $4D_{3/2}$ state. Phys. Rev. A **79**(6), 062503 (2009)
19. J. Wang, H.F. Liu, G. Yang, B.D. Yang, J.M. Wang, Determination of the hyperfine structure constants of the ^{87}Rb and ^{85}Rb $4D_{5/2}$ state and the isotope hyperfine anomaly. Phys. Rev. A **90**(5), 052505 (2014)
20. J.R. Brandenberger, R.E. Lindley, Hyperfine structure in the $6^2D_{3/2}$ and $6^2D_{5/2}$ states of ^{87}Rb and ^{85}Rb. Phys. Rev. A **91**(6), 062505 (2015)
21. S.H. Li, Y.H. Li, J.P. Yuan, L.R. Wang, L.T. Xiao, S.T. Jia, Determination of hyperfine structure constants of $5D_{5/2}$ and $7S_{1/2}$ states of rubidium in cascade atomic system. Chin. Opt. Lett. **16**(6), 060203 (2018)
22. Z.R. Wang, X.K. Hou, J.D. Bai, J.M. Wang, Measuring the hyperfine splitting and deriving the hyperfine interaction constants of the cesium $5p^67d^2D_{5/2}$ excited state. Appl. Sci. **10**(22), 8178 (2020)
23. B.D. Yang, J. Gao, T.C. Zhang, J.M. Wang, Electromagnetically induced transparency without a Doppler background in a multilevel ladder-type cesium atomic system. Phys. Rev. A **83**(1), 013818 (2011)
24. A.K. Mohapatra, T.R. Jackson, C.S. Adams, Coherent optical detection of highly excited Rydberg states using electromagnetically induced transparency. Phys. Rev. Lett. **98**(11), 113003 (2007)
25. B.D. Yang, Y. Liu, J.M. Wang, Double resonance optical pumping-polarization spectroscopy of an excited state transition. Opt. Commun. **474**, 126102 (2020)
26. C. Carr, C.S. Adams, K.J. Weatherill, Polarization spectroscopy of an excited state transition. Opt. Lett. **37**(1), 118–120 (2012)
27. B.D. Yang, J.F. Zhang, J.M. Wang, Narrow linewidth two-color polarization spectroscopy due to atomic coherence effect in a ladder-type atomic system. Chin. Opt. Lett. **17**(9), 093001 (2019)
28. J.F. Zhang, J.M. Wang, B.D. Yang, Investigation of the two-color polarization spectroscopy between the excited states based on cesium atoms. Acta Phys. Sin. **68**(11), 113201 (2019)
29. N.Ph. Georgiades, E.S. Polzik, H.J. Kimble, Two-photon spectroscopy of the $6S_{1/2}$-$6D_{5/2}$ transition of trapped atomic cesium. Opt. Lett. **19**(18), 1474–1476 (1994)
30. C. Fort, F.S. Cataliotti, P. Raspollini, G.M. Tino, M. Inguscio, Optical double-resonance spectroscopy of trapped Cs atoms: hyperfine structure of the 8s and 6d excited states. Z. Phys. D At. Mol. Clust. **34**, 91–95 (1995)
31. V. Gerginov, A. Derevianko, C.E. Tanner, Observation of the nuclear magnetic octupole moment of ^{133}Cs. Phys. Rev. Lett. **91**(7), 072501 (2003)
32. Daniel A. Steck, Cesium D Line Data, available online at http://steck.us/alkalidata (revision 2.2.1, 21 November 2019).
33. M. Tanasittikosol, C. Carr, C.S. Adams, K.J. Weatherill, Subnatural linewidths in two-photon excited-state spectroscopy. Phys. Rev. A **85**(3), 033830 (2012)